Seismic Assessment of Steel Sheet Pile Reinforcement Effect on River Embankment Constructed on a Soft Clay Ground

Kentaro NAKAI
Associate Professor, Department of Civil Engineering, Nagoya University, Nagoya, Japan
Email: nakai@civil.nagoya-u.ac.jp
Toshihiro NODA
Professor, Disaster Mitigation Research Center, Nagoya University, Nagoya, Japan
Shinji TAENAKA
Senior Researcher, Steel Structures Research Laboratories, Nippon Steel & Sumitomo Metal Corporation, Chiba, Japan
Yukihiro ISHIHARA
Manager, Press-in Technologies Support Department, GIKEN LTD., Tokyo, Japan
Nanase OGAWA
Chief, Construction Solutions Department, GIKEN LTD., Tokyo, Japan

ABSTRACT

The steel sheet pile reinforcement method is often used as a countermeasure against settlement and lateral displacement when constructing embankments on soft ground. However, it has been reported that during Kumamoto earthquake (2016), some of the sheet piles that had been installed since the construction of the embankments contributed to seismic resistance, although they were not intended as an earthquake countermeasure. Therefore, by assessing the seismic performance of the steel sheet pile method, it is also expected to expand the applicable range of the construction method. In this study, a numerical investigation on the effect of the steel sheet pile reinforcement method with different embedment lengths was conducted against dynamic loading due to earthquakes, as well as the effect of settlement and lateral displacement at the time of static loading due to embankment construction. Numerical results indicate that the steel sheet pile reinforcement method enables us to obtain not only the isolated effect for the deformation during embankment construction, but also the aseismic effect by securing the proper embedment depth.

Key words: *Soft ground, Steel sheet pile, Embedment depth, Settlement problem, Dynamic problem*

1. Introduction

When embankment construction is carried out on soft ground, settlement and lateral deformation occur in the surrounding ground induced by the consolidation settlement of the embankment (**Fig. 1(a)**). As a countermeasure method, there are two ways: (1) a method to prevent embankment from settlement by ground improvement (**Fig. 1(b)**) and (2) a method of isolating/blocking the influence (stress propagation) on the surrounding ground by walls such as steel sheet pile (**Fig. 1(c)**). In the case of constructing a new embankment, the method of (1) can reliably inhibit settlement under the embankment and the influence on the surrounding ground. However, when the soft layer is thick, the improvement cost becomes large. Although the method (2) will be less effective in inhibiting the settlement of the embankment itself, it can inhibit the deformation of the surrounding ground by installing the wall body to the supporting layer. When the weak layer is thick, it is economical and requires less space for construction compared with the ground improvement method. Therefore, this method is very effective when the structure is located in the proximity of the embankment. In order to improve the economic

efficiency, a floating pile construction method for shortening the embedment of steel sheet piles above the supporting layer has also been considered. However, it cannot be expected to inhibit ground deformation differently from the fully fixed steel sheet pile construction method. Moreover, settlement of the steel sheet pile itself is also concerned. Therefore, it is important to grasp the influence of the difference in embedment length of steel sheet pile on the deformation of the surrounding ground.

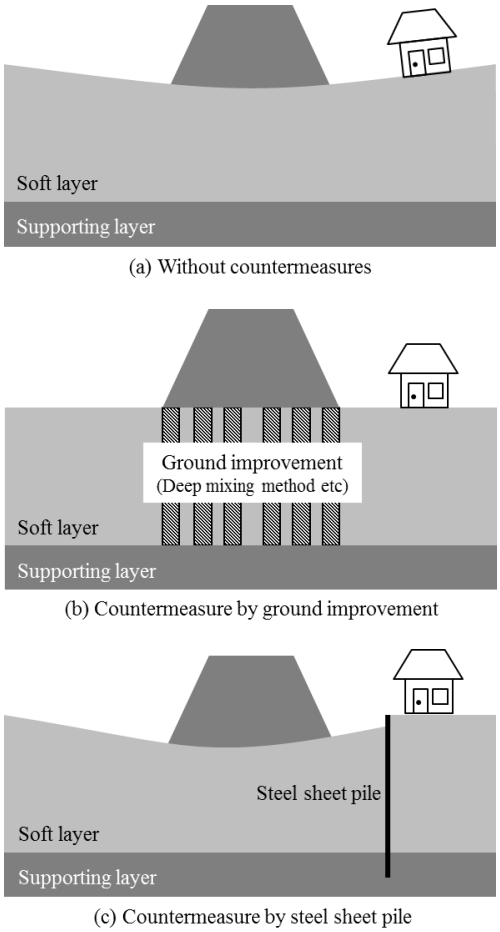

Fig. 1 Schematic drawing of general countermeasure against settlement problem

As mentioned above, the steel sheet pile method has been conventionally used as a countermeasure against static consolidation problems. However, it has been reported that during the Kumamoto earthquake (2016), some of the severed sheet piles, which had been installed during the construction of the embankments contributed to seismic resistance, although they were not intended as an earthquake countermeasure. Therefore, by assessing the seismic performance of the steel sheet pile method, it is also expected to expand the applicable range of the construction method.

In this paper, a numerical investigation on the effect of the steel sheet pile reinforcement method with different embedment lengths was conducted against dynamic loading due to earthquakes, as well as the effect of settlement and lateral displacement at the time of static loading due to embankment construction. The analysis code employed in this study is the soil-water coupled finite deformation analysis ***GEOASIA*** (Noda *et al.*, 2008), which incorporates an elasto-plastic constitutive model, namely SYS Cam-clay model (Asaoka *et al.*, 2002), that allows description of the behavior of soils ranging from sand through intermediate soils to clay within the same theoretical framework. This analysis code can be applied to both ground deformation and failure and can be used to analyse co-seismic behaviour over a time range of a few seconds to a few minutes and post-seismic behaviour, in which case the time range is from a few years to a few centuries.

2. Analysis condition

2.1. Target site

Soft ground near the mouth of the Kikuchi river in Kumamoto prefecture, Japan was targeted as a reference (Ochiai *et al.*, 1997). **Fig. 2** shows the cross section and the ground profile. It can be seen from the figure that the ground consists of 6 layers and that the N-values lies between 0 to 4 except for the SF layer at a depth of 25m. It can be therefore said that this ground is very soft.

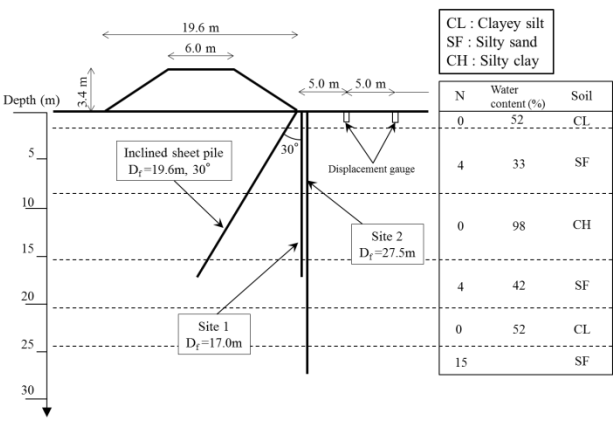

Fig. 2 Cross section and the ground profile

2.2. Finite element mesh and boundary condition

Fig. 3 shows the finite element mesh before the construction of an embankment. Only half of line symmetry is shown in the figure. The analysis region was 200 m in width and 28 m in depth. The ground was assumed to be initially horizontally layered, with an alternate layer of sand and clay. The hydraulic boundaries for the subsurface were designatedd as drained boundaries, and the bottom end and the two lateral faces were designated to be under undrained conditions. Periodic boundaries were realized by tying two nodes with the same height between both lateral ends (Noda *et al.*, 2009).

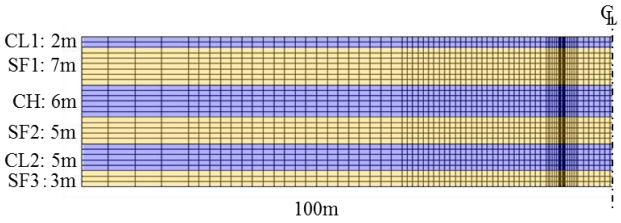

Fig. 3 Finite element mesh

2.3. Elasto-plastic properties for soils

The elasto-plastic properties (material constants and initial conditions) of the soils were all determined based on the results of mechanical tests using undisturbed samples obtained from in-situ boring surveys. The elasto-plastic properties were determined by replicating the results of these mechanical behaviors using the SYS Cam-Clay Model. The numerical simulation results of the SYS Cam-Clay model are presented in **Figs. 4**, **5**, and **6**. Mechanical properties of undisturbed samples were well replicated by the numerical simulations. **Table 1** lists the identified elasto-plastic properties. In the initial ground conditions, it was presumed that the degree of the soil skeleton structure, stress ratio and specific volume were uniform in each layer, and only the overconsolidation ratio was distributed in accordance with the overburden pressure. As for the embankment material, since the test data could not be obtained, the material constants which was used in the past research were adopted (Nakai *et al.*, 2017).

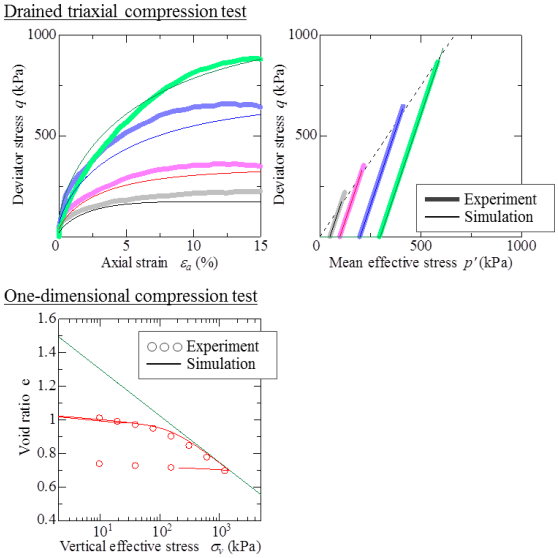

Fig. 4 Experiment & simulation result for SF layer

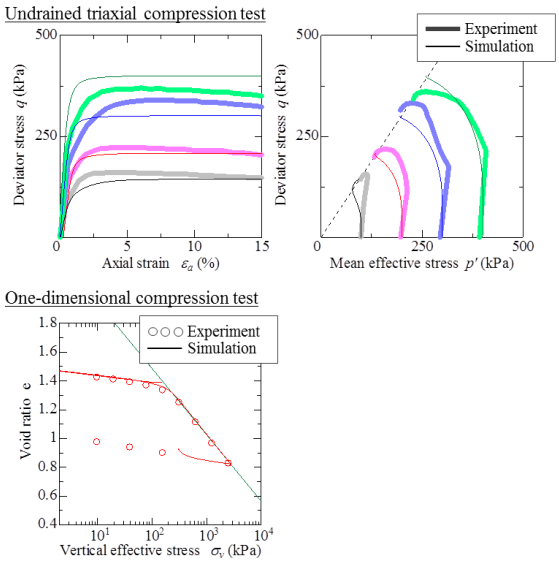

Fig. 5 Experiment & simulation result for CL layer

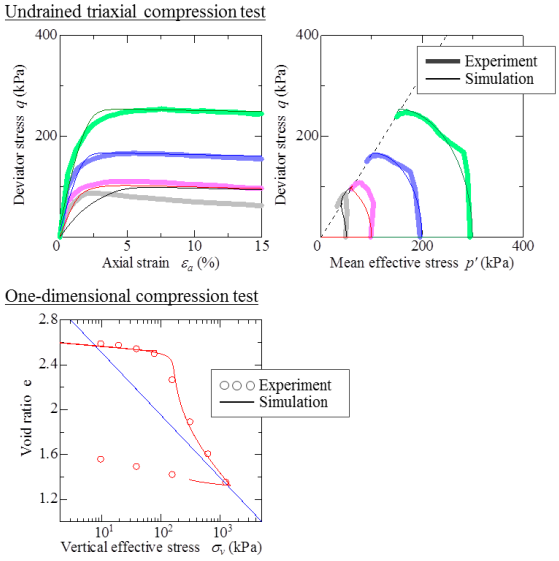

Fig. 6 Experiment & simulation result for CH layer

Table 1. Material constants and initial condition for soils

	Emb	CL	SF	CH
Elasto-plastic parameters				
Critical state index M	1.58	1.51	1.60	1.65
NCL intercept N	1.66	2.45	2.28	2.90
Compression index $\tilde{\lambda}$	0.047	0.200	0.160	0.243
Swelling index $\tilde{\kappa}$	0.0047	0.020	0.025	0.020
Poisson's ratio ν	0.30	0.20	0.20	0.40
Evolution parameters				
Degradation index of structure a	1.34	0.60	1.00	0.60
Ratio of $-D_v^p$ to $\|D_s^p\|$ c_s	1.00	0.07	1.00	0.07
Degradation index of OC m	1.28	5.00	0.80	5.00
Rotational hardening index br	0.00	0.00	0.00	0.00
Limit of rotational hardening m_b	0.00	0.00	0.0	0.00
Initial conditions				
Specific volume v	-	-	-	-
Stress ratio η_0	0.545	0.545	0.545	0.545
Degree of structure $1/R^*_0$	2.7	1.10	1.05	20.00
Degree of overconsolidation $1/R_0$	23.70	2.20	30.00	1.80
Degree of anisotropy ς_0	0.00	0.00	0.00	0.00
Soil particle density ρ_s (g/cm3)	2.65	2.65	2.65	2.65
Mass permeability index k (cm/s)	1.0×10^{-5}	1.0×10^{-6}	1.0×10^{-4}	1.0×10^{-6}

2.4. Analysis cases

Numerical analyses were carried out in the following steps.

1) A steel sheet pile was modeled by replacing the soil with a one-phase linear elastic material (**Fig. 7**) of which material constants were shown in **Table 2**. As indicated in **Table 3**, six different embedment depths of the sheet pile were considered. However, the analyses were conducted under two-dimensional plane strain conditions. Therefore, the density, Young's modulus, and yield stress were revised so that the weight, flexural rigidity, and yield moment became equivalent to the actual values.
2) Embankments 3.4 m in height with slope gradients of 2:1 were constructed on the initial ground by adding finite element meshes (Takaine et al., 2010).
3) Seismic waveform was input in the horizontal direction equally on all nodes of the bottom face of the ground. The seismic motion input was a strong motion seismogram of Kumamoto earthquake (2016) observed at K-NET station near the target area (**Fig. 8**).

Table 2. Material constants for steel sheet piles

Density ρ (g/cm3)	2.05
Poisson's ratio ν	0.3
Young's modulus E (GPa)	12.9
Yield stress σ_y (MPa)	15.1
Yield moment M_y (kNm)	860

Table 3. Analysis conditions

	Embedment depth (layer of the tip)
Case 1	No countermeasure
Case 2	5m (SF1)
Case 3	12m (CH)
Case 4	17m (SF2)
Case 5	22m (CL2)
Case 6	27m (SF3)

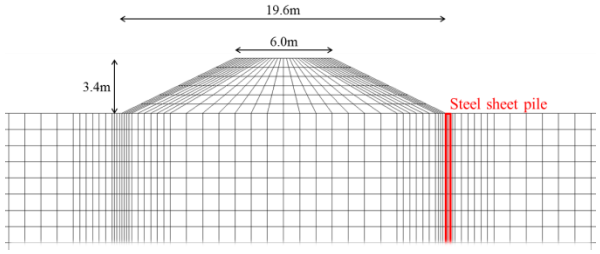

Fig. 7 Enlargement around the embankment after installation of sheet pile and construction of embankment

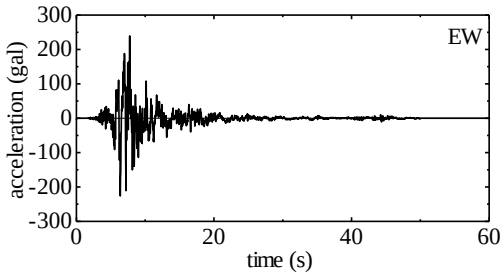

Fig. 8 Input seismic motion (Kumamoto earthquake)

3. Analysis result

3.1. Deformation by embankment construction

Figs. 9, **10** and **11** show a variation of the ground surface at different time passage. Since Cases 2, 3 and 5 show similar results to Case 4, the figures are omitted here. In the case of no countermeasures (Case 1), there is a large settlement just beneath the embankment and uplift of the surrounding ground. However, the amount of settlement below the embankment decreases due to the pile construction, and the deeper the installation is, the greater the effect is. In Case 6, when the embedment is deep enough, there were almost no deformation of the surrounding ground. In Case 4, as the pile itself sinks, settlement occurs from beneath the embankment to embankment toe, but the uplift of the surrounding ground was quite restricted. The cut-off effect, which can be

observed as a discontinuous settlement on both sides of the pile, can be reproduced even in the numerical analysis.

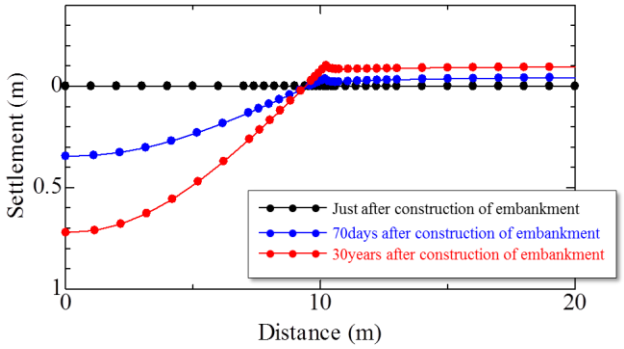

Fig. 9 Case1 (without countermeasure)

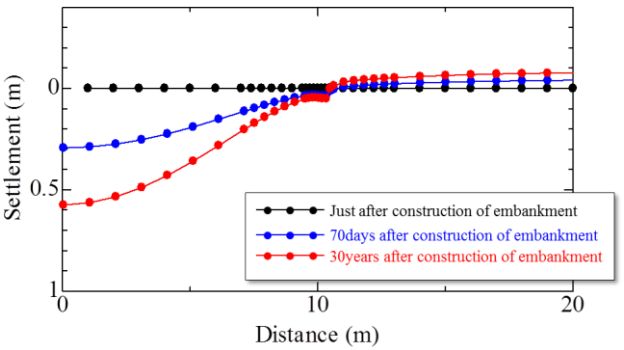

Fig. 10 Case4 (embedment depth 17m)

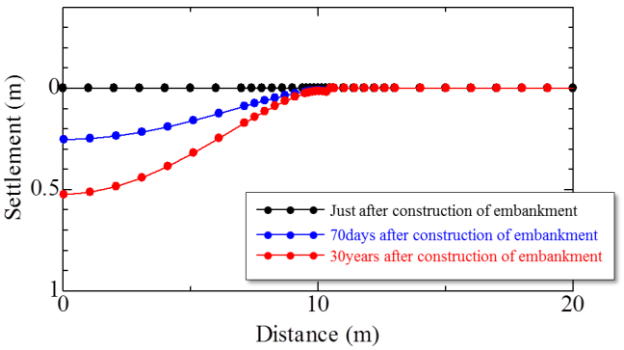

Fig. 11 Case6 (embedment depth 27m)

3.2. Deformation by seismic motion

Figs. 12 to **17** show shear strain distributions 30sec after the occurrence of an earthquake (soon after the seismic motion was finished). Although the amount of ground deformation due to embankment did not differ much from Case 2 to Case 5, the deformation at the time of the earthquake varies depending on the embedment depth of the sheet pile. When the embedment depth of the pile is shorter than 5m (Case 1 and 2), the cut-off effect by the sheet pile cannot be observed. However, when the embedment depth is longer than 12 m, as the embedment depth becomes longer, the cut-off effect appears conspicuously, and the occurrence of the shear strain of the surrounding ground is strongly inhibited. **Fig. 18** summarizes subsurface deformation 300sec after the occurrence of the earthquake. Similar to the shear strain distribution, the amount of settlement at the embankment and the deformation of the surrounding ground are large in Case 1 and Case 2. On the contrary, in Case 6, when an embedment is deep enough, both deformations become small. These numerical results indicate that the steel sheet pile reinforcement method enables to obtain the aseismic effect by securing the proper embedment depth.

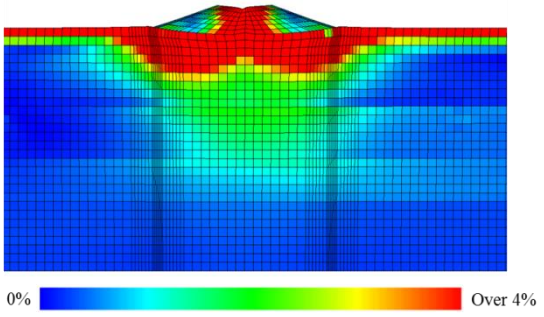

Fig. 12 Shear strain Case1 (without countermeasure)

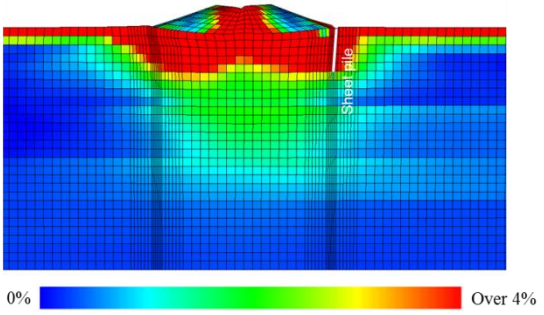

Fig. 13 Shear strain Case2 (embedment depth 5m)

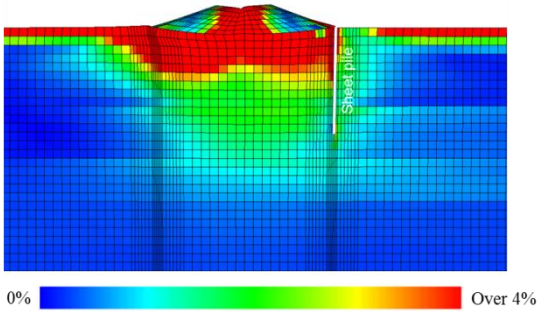

Fig. 14 Shear strain Case3 (embedment depth 12m)

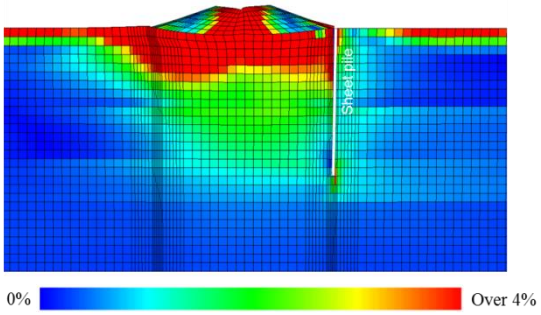

Fig. 15 Case4 Shear strain (embedment depth 17m)

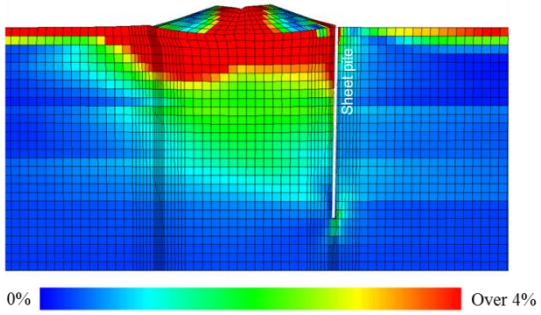

Fig. 16 Case5 Shear strain (embedment depth 22m)

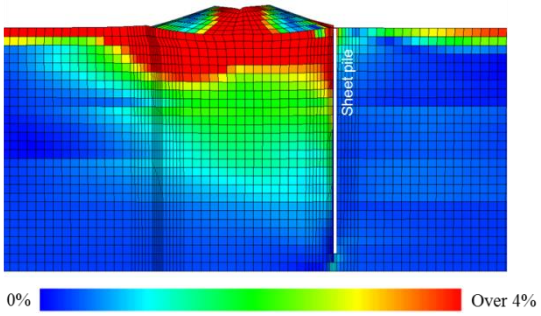

Fig. 17 Case6 Shear strain (embedment depth 27m)

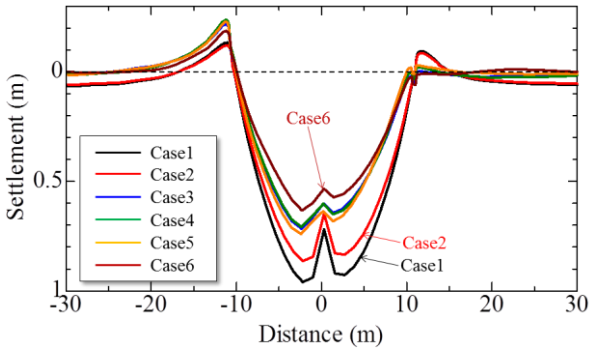

Fig. 18 Subsurface deformation with different embedment depths

4. Concluding remarks

In this study, a numerical investigation on the effect of the steel sheet pile reinforcement method with different embedment lengths was conducted against dynamic loading due to earthquakes, as well as the effect of settlement and lateral displacement at the time of static loading due to embankment construction. Numerical results indicate that the steel sheet pile reinforcement method enables us to obtain not only the cut-off effect for the deformation during embankment construction, but also the aseismic effect by securing the proper embedment depth.

5. Acknowledgements

This research was supported by International Press-in Association TC3 (Chair: Prof. Jun Otani). Authors express deep appreciation for the cooperation and useful discussion. We also thank to the National Research Institute for Earth Science and Disaster Prevention (NIED) for allowing us to use K-NET data.

References

Asaoka, A., Noda, T., Yamada, E., Kaneda, K., and Nakano, M. 2002. An elasto-plastic description of two distinct volume change mechanisms of soils. S&F, **42**(5), pp. 47–57.

Nakai, K., Noda, T. and Kato, K. 2017. Seismic assessment of river embankments reinforced by the sheet pile constructed on a low N-value soft ground, Canadian Geotechnical Journal, **54**(10), pp. 1375-1396.

Noda, T., Asaoka, A., and Nakano, M. 2008. Soil-water coupled finite deformation analysis based on a rate-type equation of motion incorporating the SYS Cam-clay model. S&F, **48**(6), pp. 771–790.

Noda, T., Takeuchi, H., Nakai, K., and Asaoka, A. 2009. Co-seismic and post-seismic behavior of an alternately layered sand-clay ground and embankment system accompanied by soil disturbance. S&F, **49**(5), pp. 739–756.

Ochiai, H., Yasufuku, N. and Otani, J. 1997. Effectiveness of sheet-pile countermeasure in soft ground. Proc of China-Japan Joint Symposium on Recent Developement of Theory & Practice in Geotechnology, Vol. 1, pp. 87-92.

Takaine, T., Tashiro, M., Shiina, T., Noda, T., and Asaoka, A. 2010. Predictive simulation of deformation and failure of peat-calcareous soil layered ground due to multistage test embankment loading. S&F, **50**(2), pp. 245–260.